ChemComm

RSCPublishing

COMMUNICATION

The Development of a Highly Photostable and Chemically Stable Zwitterionic Near-Infrared Dye for Imaging Applications

Cite this: DOI: 10.1039/x0xx00000x

Dongdong Su,[a] Chai Lean Teoh,[a] Animesh Samanta,[a] Nam-Young Kang,[a] Sung-Jin Park[a] and Young-Tae Chang*[,a,b]

Received 00th January 2014,
Accepted 00th January 2014

DOI: 10.1039/x0xx00000x

www.rsc.org/

A novel zwitterionic near-infrared (NIR) dye, ZWCC, has been designed and synthesized. It shows significantly enhanced photostability and chemical stability compared to the existing zwitterionic NIR dye. In addition, the feasibility of labeling ZWCC with biological ligands was investigated and used in live cell imaging applications.

Near-infrared (NIR) fluorophores have attracted substantial attention in various chemical and biological studies due to their great advantages for *in vivo* imaging.[1-3] Firstly, NIR wavelengths ranging from 700 nm to 900 nm can penetrate into deeper tissues. Secondly, the low auto-fluorescence background of NIR fluorophores is essential for *in vivo* images. In view of rising interests in small animal optical *in vivo* imaging, there have been high demands for the design and synthesis of novel NIR fluorophore with better photophysical properties and chemical properties.

Till now, the famous and extensively used NIR fluorophore dye, indocyanine green (**ICG**), has good clinical availability and safety properties.[3, 4] However, its low fluorescence quantum yield, short fluorescence lifetime, poor photostability, bad chemical stability, as well as the lack of reaction sites to target ligands have hindered its application in chemical and life sciences.[5] One recently developed zwitterionic NIR fluorophore **ZW800-1** shows improved *in vitro* and *in vivo* performance.[6, 7] In brief, the NIR fluorescent small molecule **ZW800-1** can be rapidly cleared by kidneys, thereby exhibiting low background fluorescence due to less non-specific binding to normal tissues and organs. Moreover, **ZW800-1** contains one carboxylic acid group, which can be modified by functional groups for covalent conjugation to target ligands through a stable amide bond.[8] However, every coin has two sides, the additional carboxylic acid, which is the reactive site for targeting ligands, was introduced by replacing chloro of meso-chloro cyclohexenyl moiety with alkoxy group via ether linkage formation.[9-12] Consequently, this molecular assembly becomes chemically less stable. When there is a strong nucleophilic group present, the reactive site containing ether linkage in cyanine dyes may undergo nucleophilic substitution at the oxygen position via a $S_{NR}1$ mechanistic pathway. Therefore, the possibility of using the **ZW800-1** dye in a harsh environment becomes limited.

Previously, Lee et al. reported the palladium-catalyzed C-C coupling reactions of chloro-substituted carbocyanines.[13] Inspired by this approach, we designed and synthesized a novel zwitterionic near-infrared fluorophore which contains a C-C cross-coupling reaction of hydrophilic chloro-substituted heptamethine cyanines with arylboronic acids. The new NIR zwitterionic C-C bond formed cross- coupling product, which we named as **ZWCC**, is not only devoid of chemically vulnerable ether linkage, but also has improved photostable characteristics. Here, we present the design and systematic study of the spectroscopic properties of this new zwitterionic NIR fluorophore (Scheme 1). Its photostability and chemical stability, as well as its application in live cell imaging are evaluated.

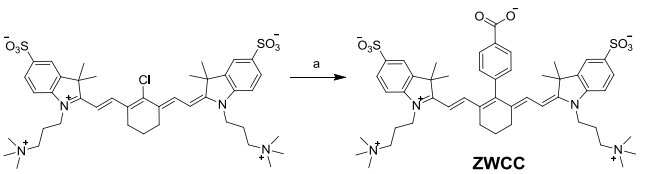

Scheme 1. General synthetic scheme. Reagents and conditions: a: 4-boronobenzoic acid, $Pd(PPh_3)_4$, K_2CO_3, H_2O, 100°C, microwave 1 h.

Spectra properties of the newly synthesized dye **ZWCC** were first tested in DMSO and compared with those of **ICG** and **ZW800-1** (Fig. 1 and Table 1). The absorption spectra of these three dyes show a characteristic band in the range of 780 -800 nm, while, the fluorescent spectra of the three compounds show some difference in emission wavelength and fluorescence intensity. Based on the same concentration, both **ZW800-1** and **ZWCC** show stronger fluorescence intensity compared to **ICG**. This is a good achievement since fluorescence intensity plays an important role in practical applications, especially in *in vivo* imaging, where higher fluorescence intensity can significantly lower the detection limit.

To further analyze and compare **ZWCC** with **ICG**, we characterized the absorption and emission spectra of these two dyes in different solvent system, such as DMSO, PBS, H_2O and MeOH. The data was summarized in Fig. S1 and Table S1. The absorption spectra of **ICG** show significant absorption peak around 780 nm in all solvent systems and significant aggregation in H_2O. For **ZWCC**, the absorption spectra are closely matched in PBS and H_2O, with a clear new absorption peak at 680 nm. However, the absorption

spectrum in DMSO shows a single peak with significant bathochromic shift, as compared to that measured in PBS.

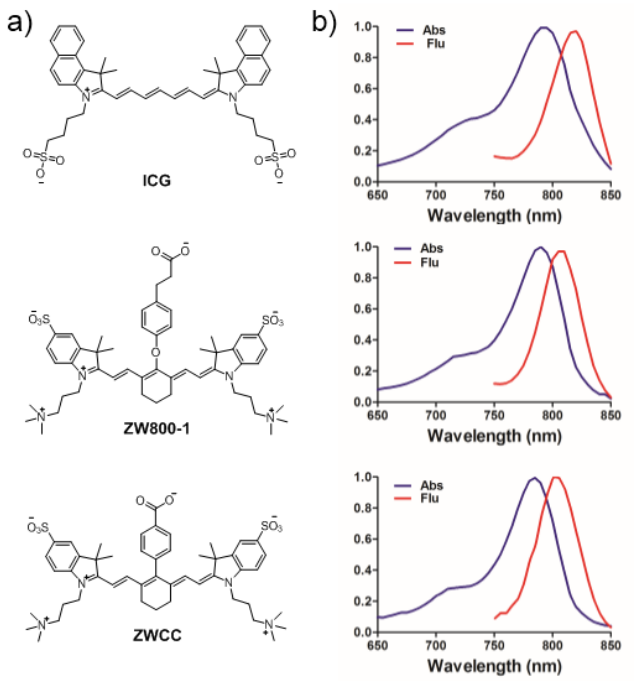

Fig. 1 (a) Chemical structures of **ICG**, **ZW800-1** and **ZWCC**; (b) Normalized absorbance and fluorescence spectra of each fluorophore (5 μM in DMSO, λ_{ex}= 730 nm).

Table 1. Comparative spectral properties of **ICG**, **ZW800-1** and **ZWCC** in DMSO.

Compound	λ_{abs} (nm)	Log ε_{max}	λ_{em} (nm)	Φ^a	$\Delta\lambda^b$
ICG	793	4.22	816	0.13	23
ZW800-1	788	5.39	807	0.36	19
ZWCC	784	5.39	806	0.44	22

[a] Fluorescence quantum yields were determined using **ICG** (Φ_f=0.13 in DMSO) as a standard.[14] [b]Stokes shifts of **ICG**, **ZW800-1** and **ZWCC**.

The aggregation tendency of **ZWCC** is evident from its absorption spectra taken in H_2O and PBS. From the area-normalized absorption spectra (equaling the concentration-weighted absorbances for different dye concentrations) shown in Fig. S2, we can see that **ZWCC** aggregates in H_2O even at concentration as low as 0.5 μM.[15] And increasing the concentrations of **ZWCC** will lead to the typically blue shift in absorption, which indicate that **ZWCC** forms the commonly observed H-type aggregation as displayed by the vast majority of cyanine-type fluorescent dyes.[15-18] The formation of non-fluorescent H-type aggregation is supported by the excitation spectra in different solvent (Fig. S3).[19, 20] Even the absorption spectra of **ZWCC** in PBS, H_2O and MeOH show clear blue-shifted absorption bands, all the excitation spectra are similar to the excitation spectra in DMSO, in which **ZWCC** does not show aggregation signal.

Quantum yield (Φ_f) is also a key parameter to evaluate the practical application of dyes. Table S1 compared the quantum yield of **ZWCC** and **ICG**, where it shows that the quantum yields of **ZWCC** in relatively different solvents are much larger than the values of **ICG** due to the good solubility of **ZWCC** in aqueous phase, which will further benefit its biological applications.

A comparative analysis for the photostability of **ICG**, **ZW800-1** and **ZWCC** dyes was carried out by performing the time-course fluorescence measurements in PBS buffer.[21, 22] First, fluorescence intensities of these dyes are examined under a strong UV lamp (UVP Blak-Ray1B-100AP high intensity mercury lamp, 100 W, 365 nm). By exposing these three compounds to a strong UV lamp and monitoring their fluorescence intensities, we observed that the average fluorescence intensity decrease for **ICG** and **ZW800-1** were around 85% and 30% due to decomposition, respectively, whereas the newly designed **ZWCC** did not show any observed decrease after 1 h irradiation (Fig. 2).

Based on the comparison, it can be concluded that **ZWCC** exhibited a remarkably higher photostability than **ICG** and **ZW800-1**. We hypothesize that the incorporation of a rigid cyclohexenyl ring in the polymethine chain increases the dye's photostability compared to cyanine dyes with an open polymethine chain. In addition, the robust C-C bond also plays an important role for enhancing the photostability of **ZWCC**.

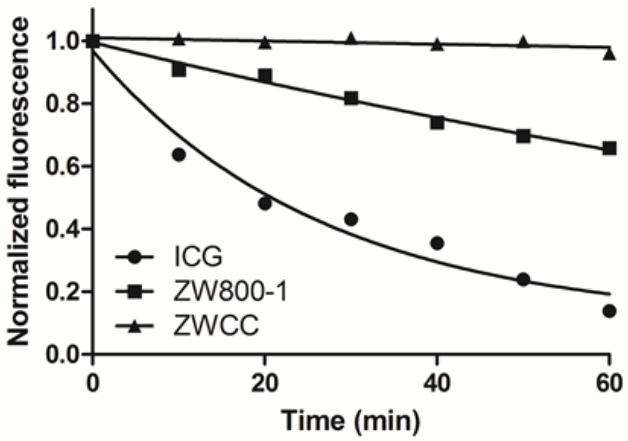

Fig. 2 Photostability evaluation of **ICG**, **ZW800-1** and **ZWCC** derivatives under strong UV irradiation. Compounds were dissolved in PBS buffer (pH 7.4) containing 1% DMSO to a 10 μM final concentration, and fluorescence measurements were recorded for 1 h at rt. Values are represented as means for sequential measurement every 10 min and fitted to a non-linear regression, one-phase exponential decay.

Besides the photostability of NIR dyes, chemical stability is also an important factor when considering further chemical modification with functional groups. First, we tested the stability of **ZWCC** under certain biological environments, like pH5 and pH10, and the results showed that **ZWCC** is stable even after 20 h incubation (Fig. S4). Both **ZW800-1** and **ZWCC** provide one carboxylic acid for further modification. We evaluated the chemical stability of **ZW800-1** and **ZWCC** by examining the nucleophilic reaction between the dyes and primary amine (Fig. S5). The HPLC-MS results show that under the same reaction condition, amide bond formation product was clearly certified for **ZWCC** with high conversion yield. On the contrary, for **ZW800-1**, only byproduct (central oxygen position replaced with amine) formation was observed (Fig. S6). These results demonstrate that the robust C-C bond provides an easier approach for modification at the single carboxylic acid linker position, leading to the superior chemical stability of **ZWCC** even under harsh environment.

Signal-to-noise (S/N) ratio is a significant criterion for bioimaging. To evaluate the S/N ratio of **ZWCC**, **ZWCC** was injected to BALB/c nude mouse and the animal was imaged. It is clear from the images that **ZWCC** was distributed to organs including liver, pancreas, kidneys, spleen, intestine and fat pad. Subsequently, the signal quickly disappeared from the liver, pancreas, spleen, intestine and fat pad. Within 1 h, fluorescence signal has mostly cleared from the whole body and only very weak

signal remained to be observed in the kidneys and bladder, which indicated the low background of **ZWCC** (Fig. S7).

To further demonstrate the feasibility of labeling biological ligands, we conjugated the new zwitterionic NIR fluorophore **ZWCC** to a cyclic peptide consisting of cyclo (RGDyK) (cRGD), which shows specifically binding to integrin αvβ3. Integrins are expressed on a wide variety of cells to mediate cell-extracellular matrix interactions and the integrin receptor, αvβ3, in particular is an angiogenic marker expressed in most regions of tumors.[23] Several potent small molecules containing the arginine-glycine-aspartate (RGD) sequence have been found to block integrin function and inhibit tumor angiogenesis.[24] These promising results have suggested that integrin receptors are important targets for drug delivery and therapy, as well as molecular imaging.

a)

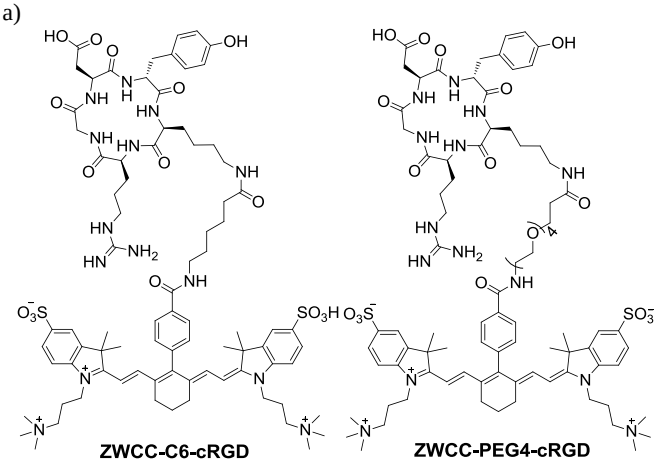

b)

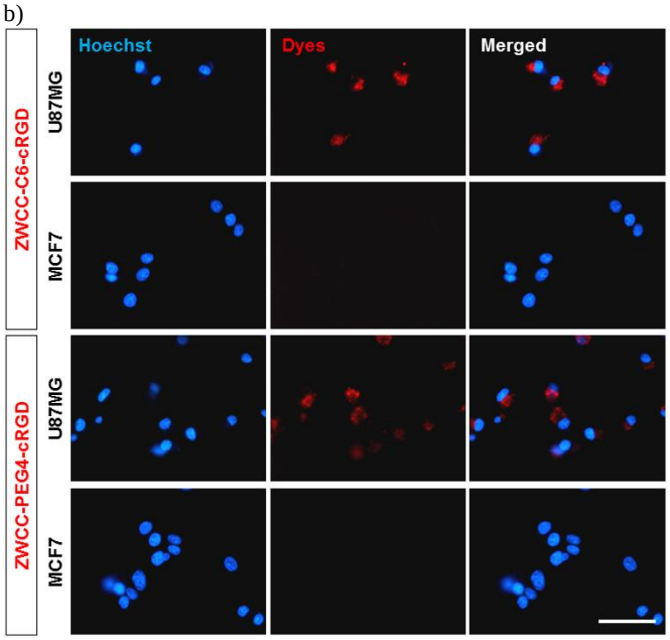

Fig. 3. Structures (a) and fluorescence cell imaging of **ZWCC**-linker-cRGD (b). Red colour is from **ZWCC** compounds (middle panels) and blue colour is from Hoechst stain (left panels) for nuclei visualization. Right panels show merged images of the two. Images were captured by 40x objective. Scale bar is 50 μm.

We synthesized two cRGD-conjugated **ZWCC** compounds as possible probes for monitoring tumor angiogenesis. We evaluated integrin-targeting and cellular uptake of cRGD-conjugated **ZWCC** compounds by fluorescence imaging analysis using αvβ3 integrin-positive U87MG cells and αvβ3 integrin-negative MCF7 cells. As shown in Fig. 3, both **ZWCC-C6-cRGD** and **ZWCC-PEG4-cRGD** were internalized by U87MG cells during the incubation period. As a negative control, incubating all three integrin-targeted **ZWCC** compounds did not yield any signals in αvβ3 integrin-negative MCF7 cells. Similarly, no signal was observed when cells were treated with **ZWCC** alone (data not shown). In addition, the fluorescent signal from **ZWCC**-linker-cRGD could be effectively inhibited when U87MG cells were pre-treated with free cRGD peptide, indicating the specificity of **ZWCC**-linker-cRGD binding to integrin αvβ3 (Fig. S8).

In summary, we have developed a novel zwitterionic NIR dye, **ZWCC**, which shows significantly enhanced photostability as well as chemically stable properties. Also, based on their functional carboxylic acid group, we designed and constructed two cRGD-modified NIR probes which demonstrated specific integrin-targeting in live cells. Taken together, we anticipate that the newly developed zwitterionic NIR dye, **ZWCC**, will offer a better and improved option in the field of NIR imaging.

We gratefully acknowledge the intramural funding from A*STAR (Agency for Science, Technology and Research, Singapore) Biomedical Research Council and National Medical Research Council grant (NMRC/CBRG/0015/2012).

Notes and references

[a] Singapore Bioimaging Consortium, Agency for Science, Technology and Research (A*STAR), 138667, Singapore.

[b] Department of Chemistry & MedChem Program of Life Sciences Institute, National University of Singapore, 117543

† Electronic Supplementary Information (ESI) available: Experimental details, spectra, cell image and HPLC-MS. See DOI: 10.1039/c000000x/

1. J. Fabian, H. Nakazumi and M. Matsuoka, *Chem. Rev.*, 1992, **92**, 1197-1226.
2. E. M. Sevick-Muraca, J. P. Houston and M. Gurfinkel, *Curr. Opin. Chem. Biol.*, 2002, **6**, 642.
3. J. V. Frangioni, *Curr. Opin. Chem. Biol.*, 2003, **7**, 626.
4. S. Kobayashi and A. Makino, *Chem. Rev.*, 2009, **109**, 5288.
5. J. O. Escobedo, O. Rusin, S. Lim and R. M. Strongin, *Curr. Opin. Chem. Biol.*, 2010, **14**, 64.
6. H. S. Choi, K. Nasr, S. Alyabyev, D. Feith, J. H. Lee, S. H. Kim, Y. Ashitate, H. Hyun, G. Patonay, L. Strekowski, M. Henary and J. V. Frangioni, *Angew. Chem. Int. Edit.*, 2011, **50**, 6258.
7. H. S. Choi, S. L. Gibbs, J. H. Lee, S. H. Kim, Y. Ashitate, F. Liu, H. Hyun, G. Park, Y. Xie, S. Bae, M. Henary and J. V. Frangioni, *Nat. Biotech.*, 2013, **31**, 148.
8. S. H. Kim, J. H. Lee, H. Hyun, Y. Ashitate, G. Park, K. Robichaud, E. Lunsford, S. J. Lee, G. Khang and H. S. Choi, *Sci. Rep.*, 2013, **3**, 1198.
9. W. Pham, Z. Medarova and A. Moore, *Bioconjug. Chem.*, 2005, **16**, 735.
10. S. A. Hilderbrand, K. A. Kelly, R. Weissleder and C. H. Tung, *Bioconjug. Chem.*, 2005, **16**, 1275.
11. L. Strekowski, M. Lipowska and G. Patonay, *J. Org. Chem.*, 1992, **57**, 4578.
12. M. Matsui, Y. Hashimoto, K. Funabiki, J.-Y. Jin, T. Yoshida and H. Minoura, *Synthetic Metals*, 2005, **148**, 147.
13. H. Lee, J. C. Mason and S. Achilefu, *J. Org. Chem.*, 2006, **71**, 7862.
14. K. Licha, B. Riefke, V. Ntziachristos, A. Becker, B. Chance and W. Semmler, *Photochem. Photobiol.*, 2000, **72**, 392.
15. J. Pauli, K. Licha, J. Berkemeyer, M. Grabolle, M. Spieles, N. Wegner, P. Welker and U. Resch-Genger, *Bioconjug. Chem.*, 2013, **24**, 1174.
16. M. Grabolle, R. Brehm, J. Pauli, F. M. Dees, I. Hilger and U. Resch-Genger, *Bioconjug. Chem.*, 2012, **23**, 287.
17. E. Arunkumar, N. Fu and B. D. Smith, *Chem. Eur. J.*, 2006, **12**, 4684.
18. C. Haritoglou, A. Gandorfer, M. Schaumberger, R. Tadayoni, A. Gandorfer and A. Kampik, *Invest. Ophthalmol. Vis. Sci.*, 2003, **44**, 2722.

19. N. Marmé, G. Habl and J.-P. Knemeyer, *Chem. Phys. Lett.*, 2005, **408**, 221.
20. Z. Zhang, M. Y. Berezin, J. L. Kao, A. d'Avignon, M. Bai and S. Achilefu, *Angew. Chem. Int. Edit.*, 2008, **47**, 3584.
21. A. Samanta, M. Vendrell, R. Das and Y. T. Chang, *Chem. Commun.*, 2010, **46**, 7406.
22. R. K. Das, A. Samanta, H.-H. Ha and Y.-T. Chang, *RSC Adv.*, 2011, **1**, 573.
23. G. Niu and X. Chen, *Theranostics*, **1**, 30-47.
24. A. Carter, *J. Natl. Cancer. Inst.*, **102**, 675-677.

TOC

ZWCC, a new zwitterionic NIR dye with high photostability and enhanced chemical stability, can be easily functionalized for biological applications.

The Development of a Highly Photostable and Chemically Stable Zwitterionic Near-Infrared Dye for Imaging Applications

Dongdong Su,[a] *Chai Lean Teoh,*[a] *Animesh Samanta,*[a] *Nam-Young Kang,*[a] *Sung-Jin Park*[a] *and Young-Tae Chang**[,a,b]

[a] Singapore Bioimaging Consortium, Agency for Science, Technology and Research (A*STAR), 138667, Singapore.

[b] Department of Chemistry & MedChem Program of Life Sciences Institute, National University of Singapore, 117543, Singapore

List of Contents

Experimental Procedures

Material and Method

All reactions were performed in oven-dried glassware under a positive pressure of nitrogen. Unless otherwise noted, starting materials and solvents were purchased from Aldrich and Acros organics and used without further purification. c(RGDyK) was purchased from ChinaPeptides Co., Ltd. NMR spectra were recorded on a Bruker AMX500 (500 MHz) NMR spectrometer. Chemical shifts are reported as δ in units of parts per million (ppm) and coupling constants are reported as a *J* value in Hertz (Hz). Mass of all the compounds was determined by LC-MS of Agilent Technologies with an electrospray ionization source.

Spectroscopic and quantum yield data were measured on a SpectraMax M2 spectrophotometer (Molecular Devices). Data analysis was performed using Graph Prism 5.0.

Quantum Yield Measurements

Quantum yields for all the fluorescent compounds were measured by dividing the integrated emission area of their fluorescent spectrum against the area of **ICG** in DMSO excited at 730 nm (Φ_{ICG} = 0.13).[1] Quantum yields where then calculated using equation (1), where *F* represents the integrated emission area of fluorescent spectrum, η represents the refractive index of the solvent, and *Abs* represents absorbance at excitation wavelength selected for standards and samples. Emission was integrated from 750 nm to 850 nm.

$$\Phi_{flu}^{sample} = \Phi_{flu}^{reference}\left(\frac{F^{sample}}{F^{reference}}\right)\left(\frac{\eta^{sample}}{\eta^{reference}}\right)\left(\frac{Abs^{reference}}{Abs^{sample}}\right) \quad (1)$$

Photostability Experiment

Strong UV Lamp Procedure: 1 nmol compounds in 96-well black plate was added 1 μL DMSO and followed by 99 μL PBS buffer (pH 7.4). The final concentrations of compounds were 10 μM. Fluorescence intensity measurements were carried out in each 10 min interval for a total period of 1 h (λ_{ex}= 760 nm, λ_{em}= 800 nm). UV lamp: UVP Blak-Ray1B-100AP high intensity mercury lamp, 100 W, 365 nm).

Cell Culture and Imaging Experiments

U87MG and MCF7 cells were cultured in high-glucose (4500 mg/L) containing-Dulbecco's Modified Eagle's medium (DMEM) supplemented with 10 % fetal bovine serum, 100 U/ml penicillin and 100 µg/ml streptomycin. 24-36 h prior to imaging, cells were seeded in clear bottom, 96-well plate. **ZWCC** compounds were added to cultured cells to reach final concentration of 5 µM and incubated for 4-6 h at 37 ºC. Cells were washed with PBS buffer twice before imaging. To confirm that ZWCC-linker-cRGD binds specifically to integrin αvβ3, U87MG cells were incubated with 10 µM RGD before ZWCC-linker-cRGD were added. Live cells images were acquired on an inverted Ti-E microscope (Nikon Instruments Inc), equipped with a customised Ex 750 nm/ Em 800 nm filter for NIR fluorescence acquisition, as well as DAPI for Hoechst33342 fluorescence acquisition. Images were analysed using NIS Elements 3.10 software.

In Vivo Bio-distribution of ZWCC dyes in BALB\c nude mice

BALB/c nude mice (18 - 20 g) were obtained from the Biological Resource Centre (Biomedical Sciences Institutes) and anesthetized by intraperitoneal injection of ketamine (150 mg/kg)/xylazine (10 mg/kg) at 8 weeks of age. The mice were placed under the microscope before the survival surgery. An anesthetic gas (Isofluorane) was maintained during bio-distribution study for 1 h. The **ZWCC** (500 µM x 100 µL in saline containing 1% of PEG, 0.1% of tween20, 10 µL/g, and 1% DMSO) were injected intravenously (i.v.) after capturing the first images as a control. Time dependent fluorescence images were acquired with a Leica M205 FA Fluorescent Stereo Microscope using a 3.95X objective lens with a NIR camera, measured and processed with NIS-Elements 3.10.

Chemical Synthesis

Synthesis of **ZWCC:** Precursor chloro dye was synthesized as reported.[2] Precursor chloro dye (60 mg, 0.074 mmol) and 4-carboxyphenylboric acid (24.5 mg, 0.147 mmol) in H_2O were reacted in microwave reactor in the presence of a catalytic amount of $Pd(PPh_3)_4$ and K_2CO_3 for 1 h. After reaction, the mixture was washed with anhydrous ethyl acetate, and the water phase was separated and dried under reduced pressure. The crude product was further purified by HPLC (yield: 45%).

^{1}H NMR (500 MHz, CH_3CN+D_2O): δ 8.89 (s, 1H), 8.69 (d, J = 7.8 Hz, 2H), 8.22 (d, J = 8.3 Hz, 2H), 8.19 (s, 1H), 7.65 (s, 1H), 7.62 (d, J = 7.3 Hz, 2H), 7.51 (d, J = 8.3 Hz, 2H), 6.65 (d, J = 13.9 Hz, 2H), 6.01 (s, 1H), 4.35 (t, J = 6.8 Hz, 4H), 3.97 – 3.87 (m, 4H), 3.58 (s 18H), 3.26 (m, 4H), 2.67 – 2.42 (m, 6H), 1.54 (s, 12H).

^{13}C NMR (126 MHz, CH_3CN+D_2O): δ 172.79, 171.29, 163.43, 149.42, 143.47, 142.24, 141.37, 141.10, 135.08, 134.40, 133.72, 130.32, 129.53, 129.09, 127.43, 120.26, 110.91, 101.26, 63.45, 53.53, 48.91, 40.94, 27.38, 24.81, 21.22.

HRMS *m/z* ($C_{49}H_{62}N_4O_8S_2$) calculated: 898.4009, found: $(M+Na)^+$ 921.3874.

Scheme S1. General synthetic scheme of **ZWCC-linker-cRGD**.

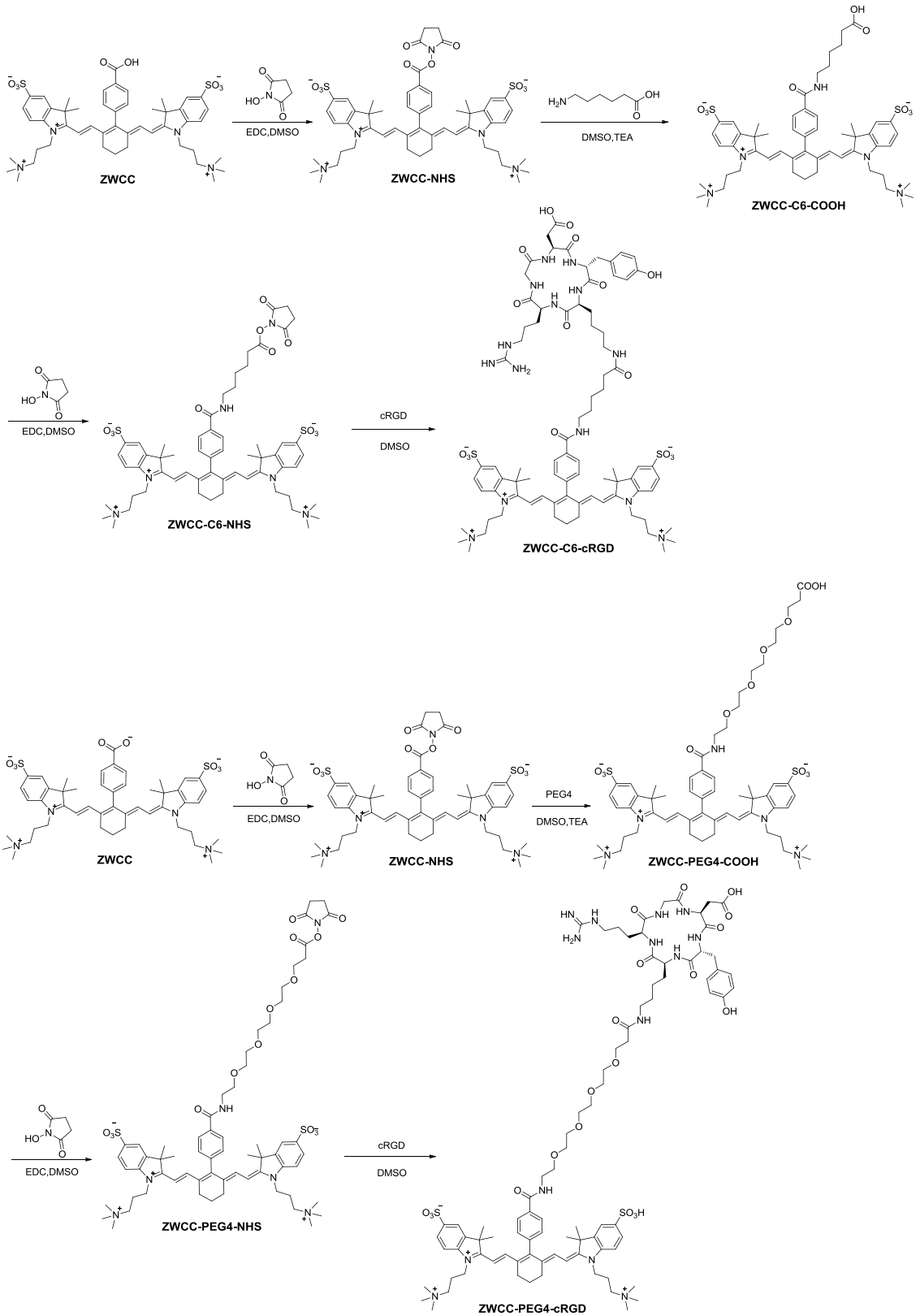

Synthesis of **ZWCC-NHS**, **ZWCC-C6-NHS** and **ZWCC-PEG4-NHS**: Each of relevant acid (1 equiv) was mixed with N-Hydroxysuccinimide (3 equiv), EDC (3 equiv) in DMSO. The mixture was stirred at room temperature and the reaction was monitored using LCMS. After reaction, collect the solid after adding enough anhydrous ethyl acetate to the reaction mixture. The product was used for the next step without further purification. All compounds were confirmed by HPLC-MS.

Synthesis of **ZWCC-C6-COOH** and **ZWCC-PEG4-COOH**: **ZWCC-NHS** (1 equiv) was mixed with each of linker (2 equiv), TEA (2 equiv) in DMSO. The mixture was stirred at room temperature for 2 h. After reaction, collect the solid after adding enough anhydrous ethyl acetate to the reaction mixture. The crude product was purified by HPLC to afford the corresponding compounds as green solid. All compounds were confirmed by HPLC-MS.

Synthesis of **ZWCC-C6-cRGD** and **ZWCC-PEG4-cRGD**: Each of NHS ester (1 equiv) was mixed with **cRGD** (2 equiv), TEA (2 equiv) in DMSO. The mixture was stirred at room temperature for 2 h. After reaction, collect the solid after adding enough anhydrous ethyl acetate to the reaction mixture. The crude product was purified by HPLC to afford the corresponding compounds as green solid. All compounds were confirmed by HPLC-MS.

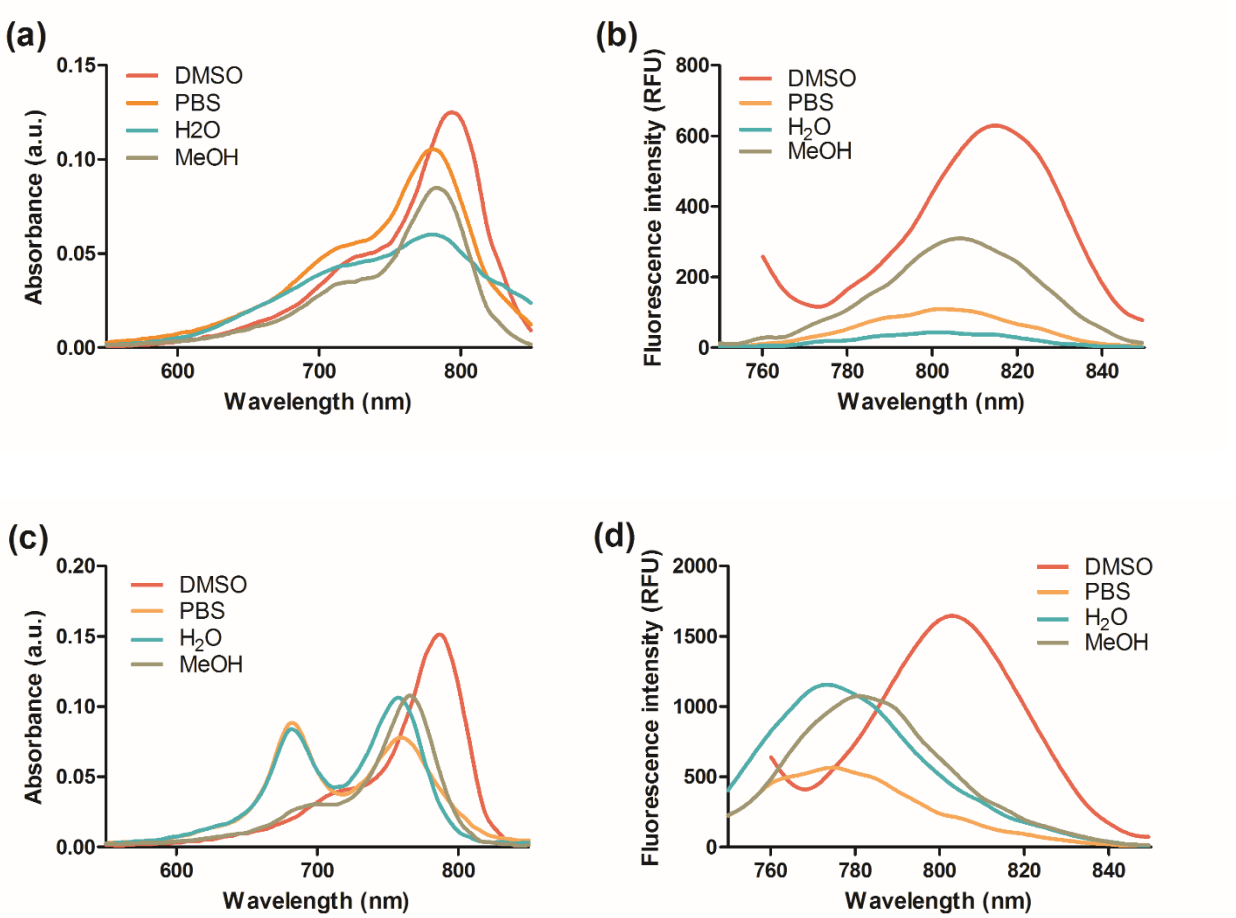

Figure S1. Absorption and emission spectra of **ICG** (a and b) and **ZWCC** (c and d) in different solvent systems at a concentration of 5 μM (λ_{ex}= 730 nm).

Table S1. Photophysical data of **ICG** and **ZWCC** in various aqueous buffers and organic solvents.

	Solvent	λ_{abs} (nm)	ε_{max}	λ_{em} (nm)	Φ^a	$\Delta\lambda^b$
ICG	DMSO	793	218000	816	0.13	21
	PBS	780	184000	802	0.04	22
	H_2O	780	105000	801	0.01	21
	MeOH	783	148000	806	0.08	23
ZWCC	DMSO	784	263000	806	0.44	22
	PBS	758	136000	774	0.28	16
	H_2O	757	184000	773	0.21	16
	MeOH	766	188000	781	0.24	15

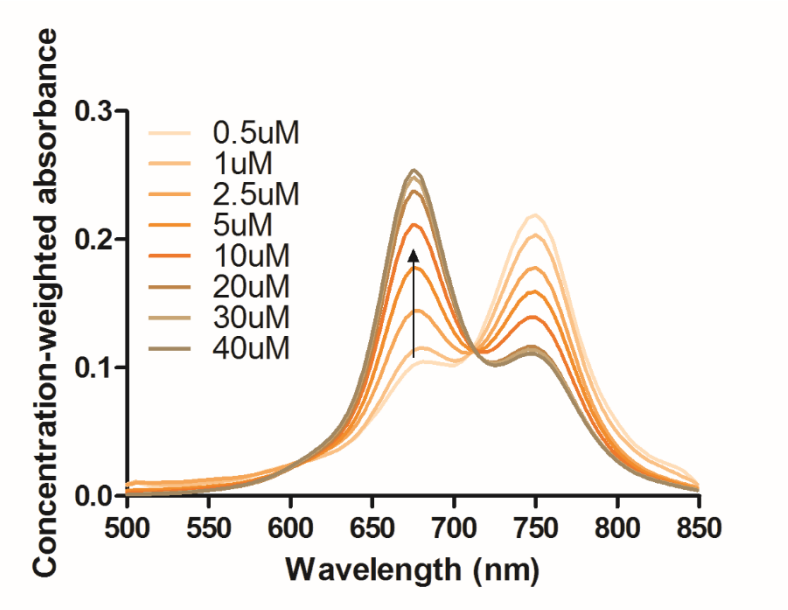

Figure S2. Concentration-weighted absorption spectra of **ZWCC** measured at different dye concentrations between 0.5 − 40 µM in H_2O.

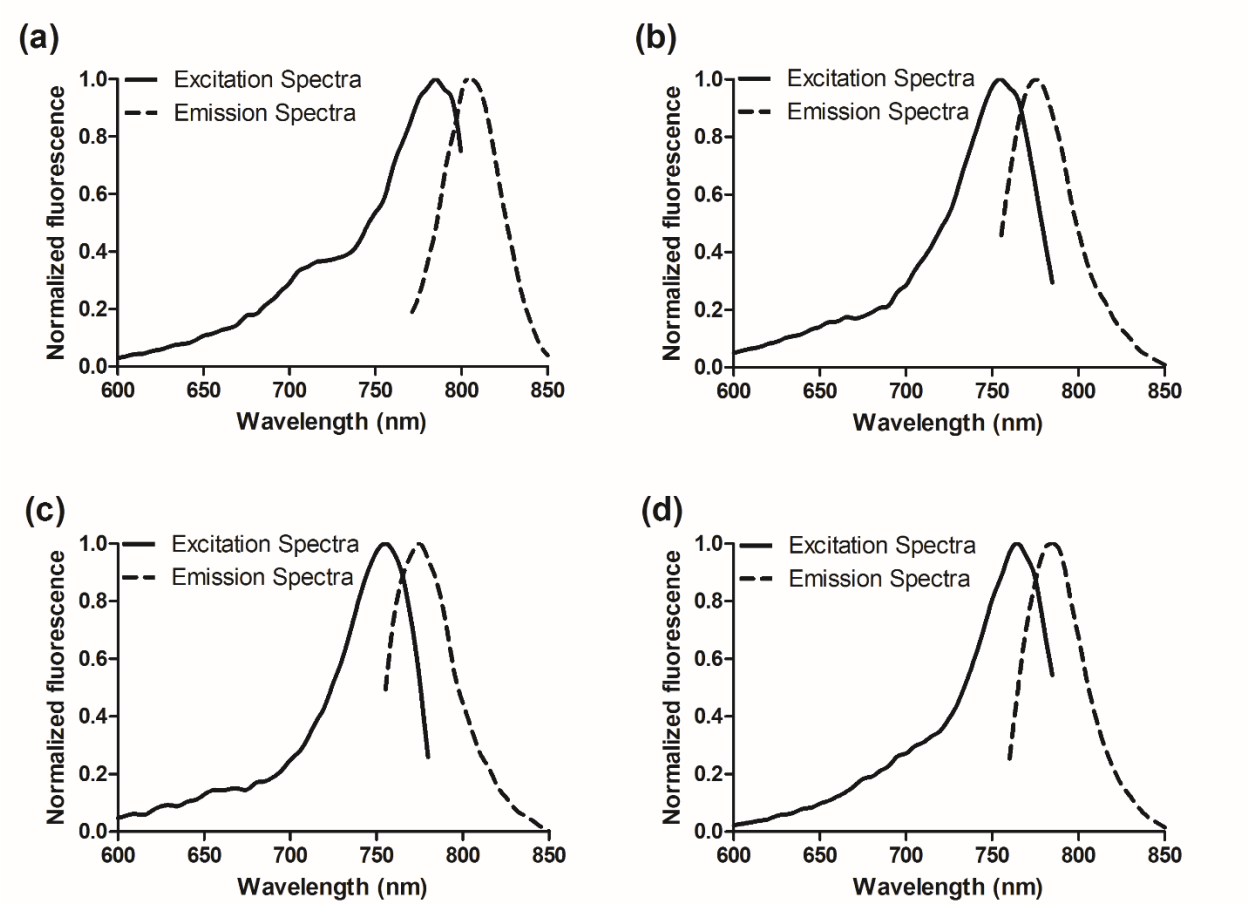

Figure S3. Normalized Excitation and emission spectra of **ZWCC** (5 μM) in 4 different solvent system (λ_{ex}= 730 nm) (a) DMSO, (b) PBS, (c) H_2O, (d) MeOH.

(a)

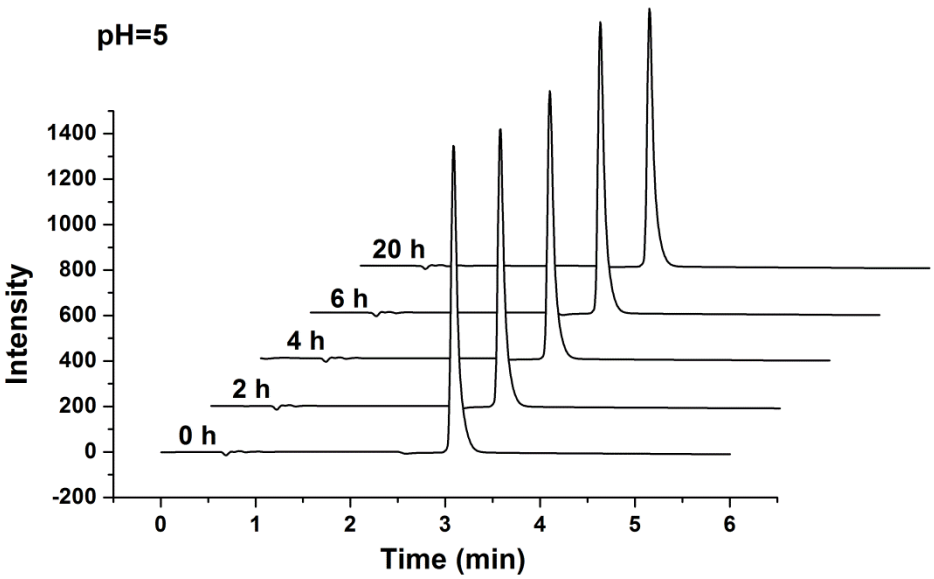

(b)

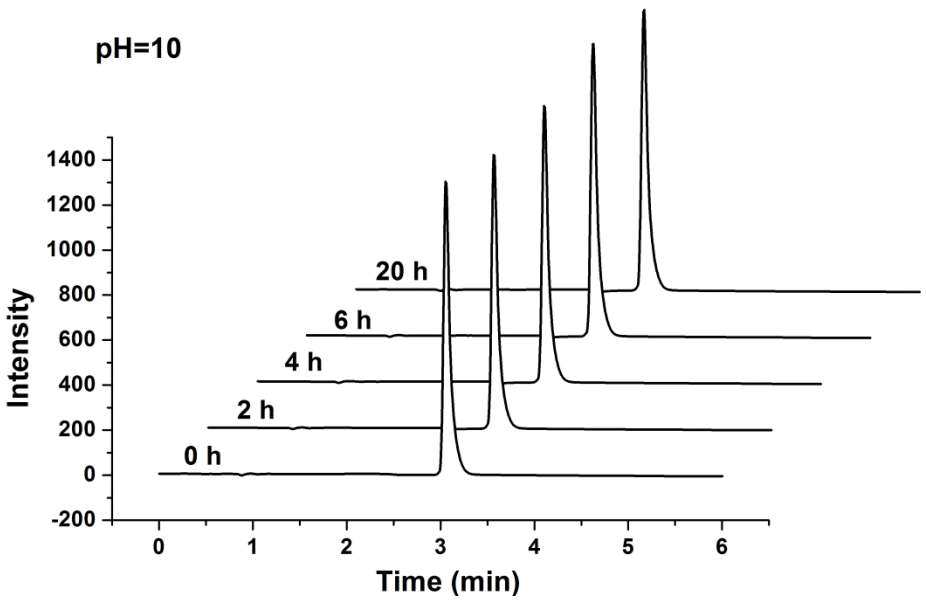

Figure S4. Chemical stability of **ZWCC** under pH 5 (a) and pH 10 (b), UV detection: 700 nm.

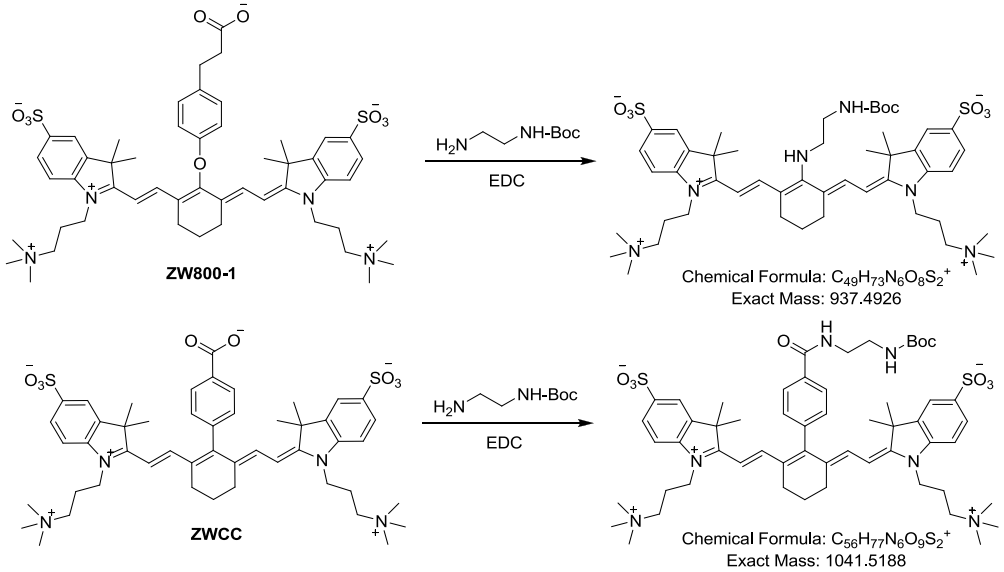

Figure S5. Chemical reaction activity of **ZW800-1** and **ZWCC** with primary amine. Reaction condition: DMF:DMSO=4:1, rt, 4 h.

(a) LCMS data for reaction of **ZWCC** and tert-butyl 2-aminoethylcarbamate.

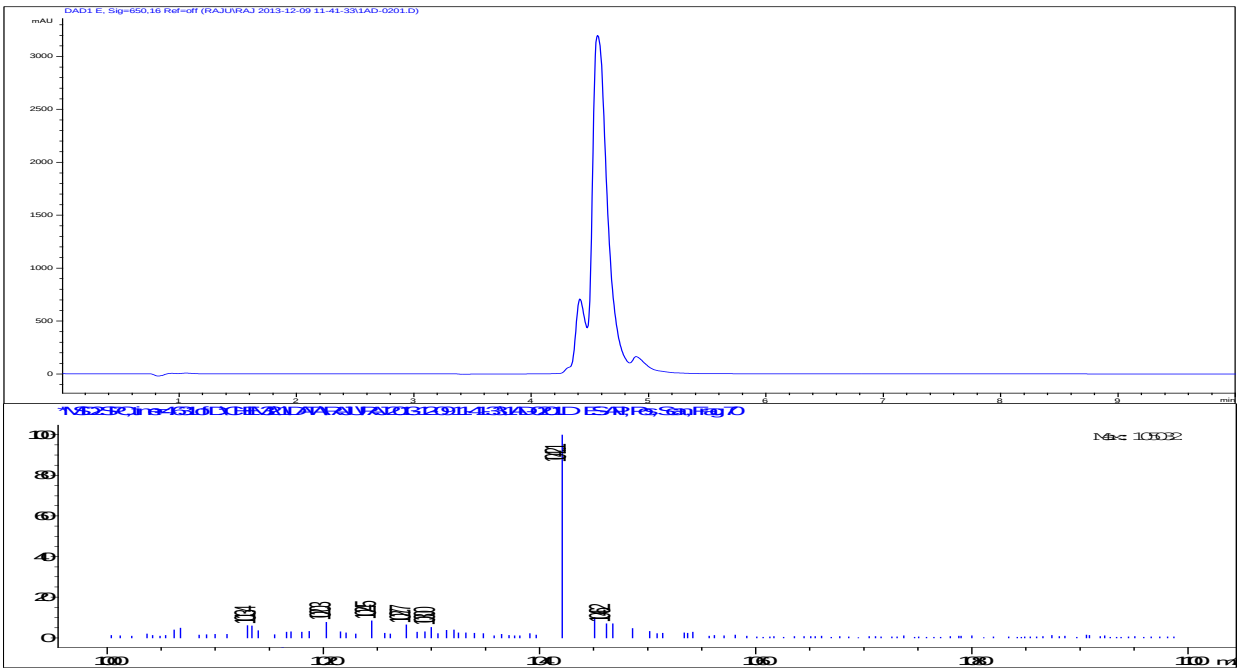

(b) LCMS data for reaction of **ZW800-1** and tert-butyl 2-aminoethylcarbamate.

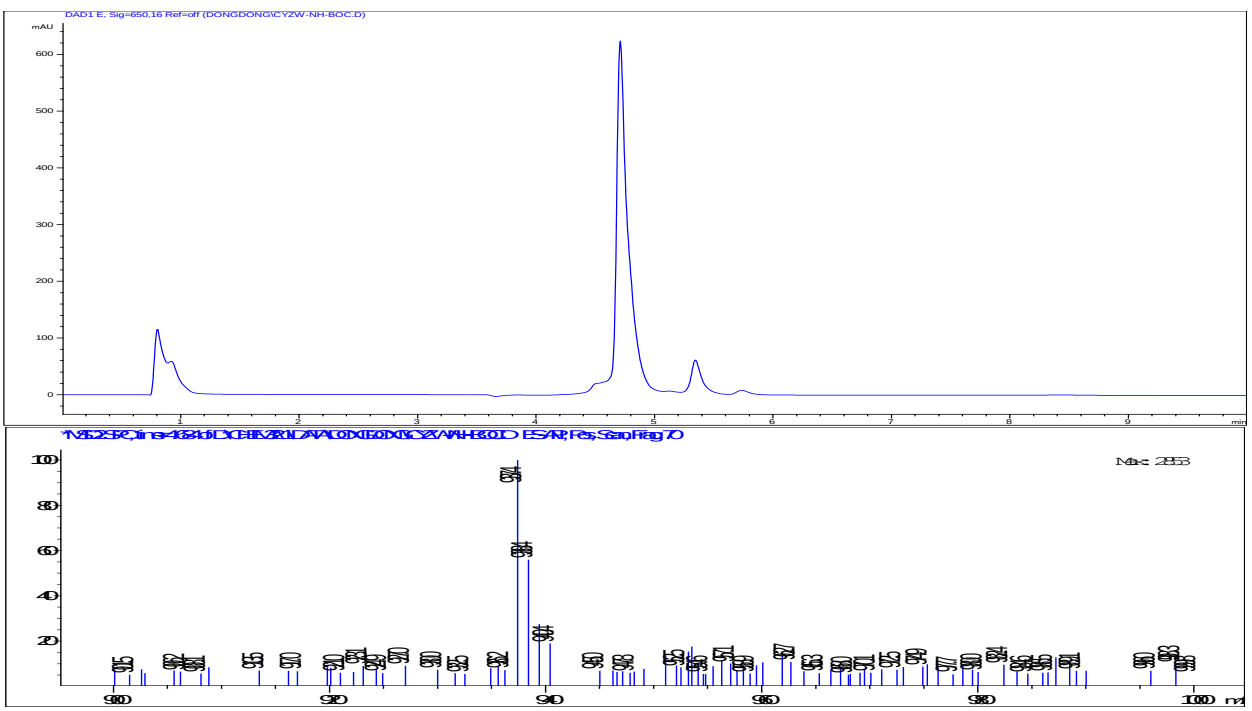

Figure S6. Reverse-phase HPLC monitoring of reaction after 4 h. (UV detection: 650 nm, MS detection: ESI-MS).

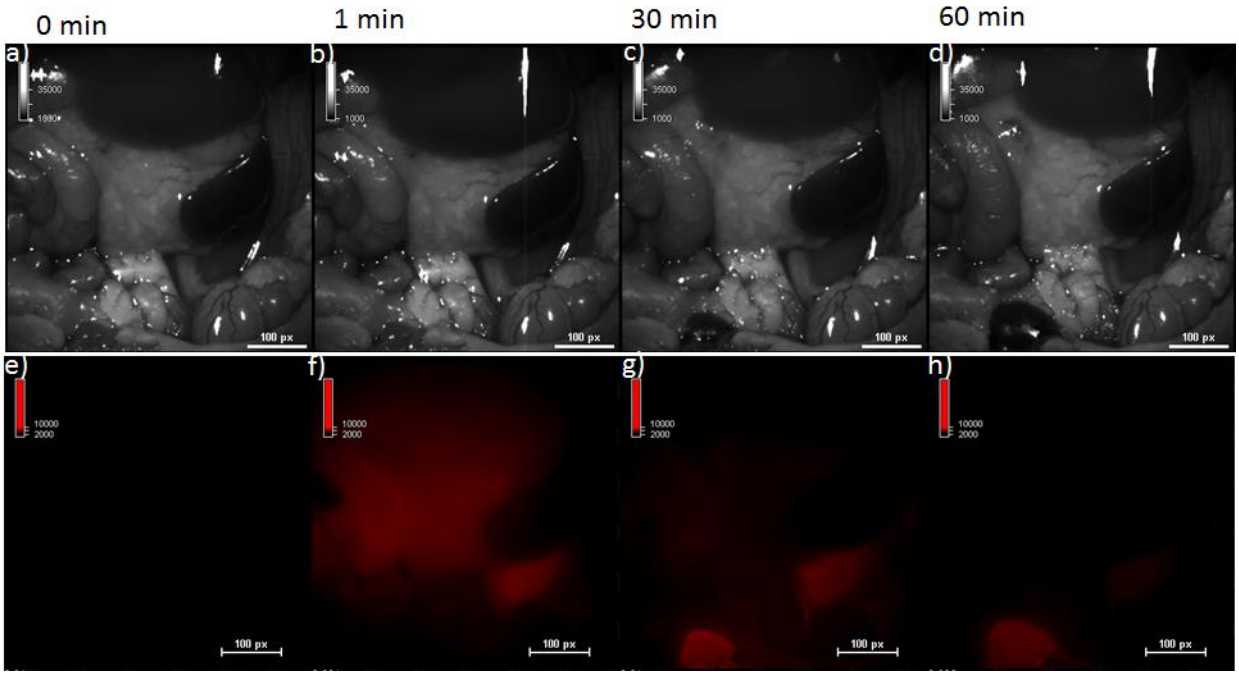

Figure S7. Biodistribution and clearance of **ZWCC** in BALB/c nude mouse in vivo. Bright field and fluorescence images (NIR camera) were captured after and before the injection of ZWCC dye through tail vain. a) & e) before the injection of dyes. b) & f) 1 min after the injection c) & g) after 30 min and d) & h) after 60 min of post injection respectively. 100 μL of 500 μM **ZWCC** dye in PBS buffer containing 1% of PEG, 0.1% of tween20, 10 μL/g, and 1% DMSO was injected.

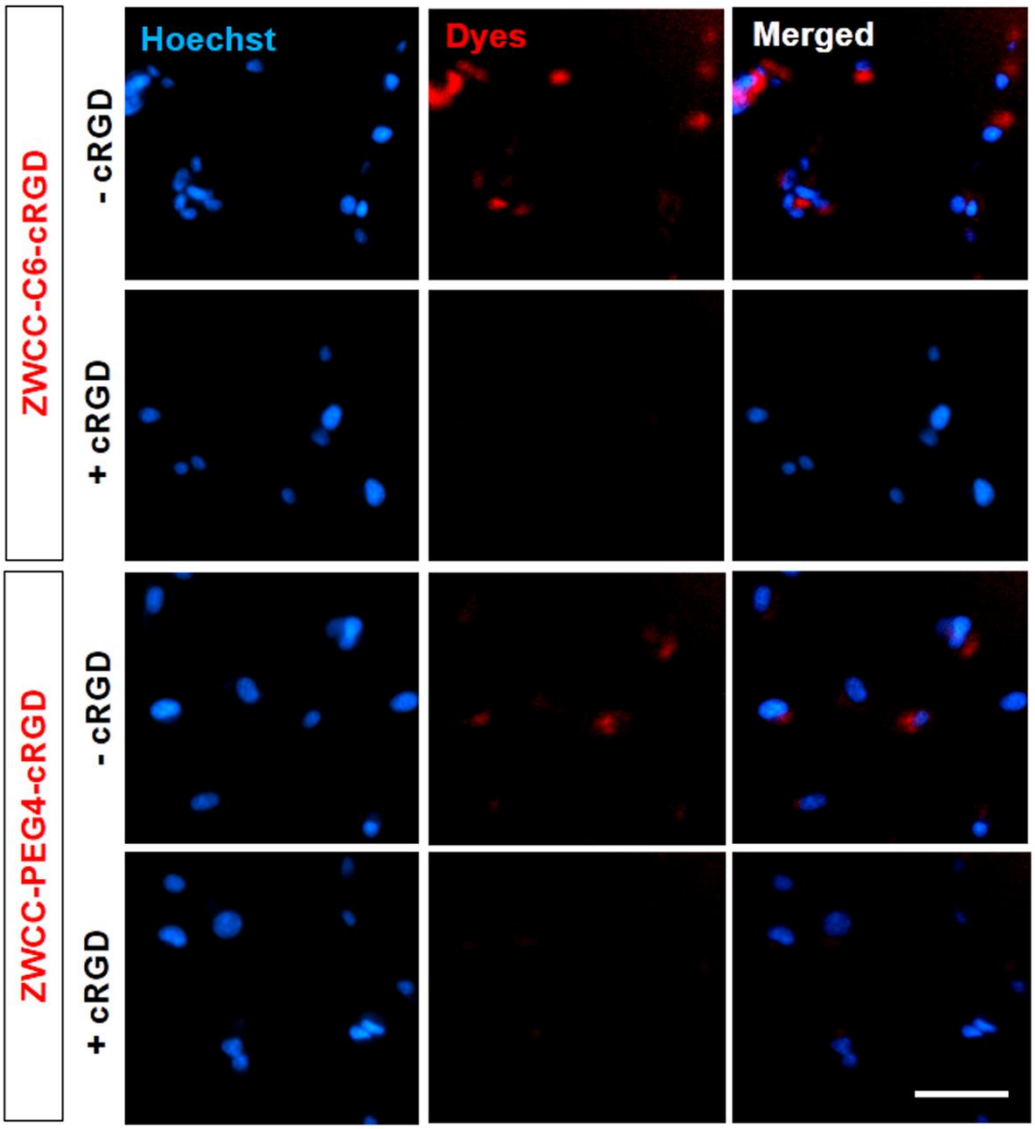

Figure S8. Fluorescence staining of **ZWCC-linker-cRGD** in integrin αvβ3 positive cells. Lower panels show blocking by free **cRGD** before staining by **ZWCC-linker-cRGD**. Red colour is from **ZWCC** compounds (middle panels) and blue colour is from Hoechst stain (left panels) for nuclei visualization. Merged images of the two are shown in the right panels. Images were captured on a 20x objective. Scale bar is 100 μm.

HPLC-MS

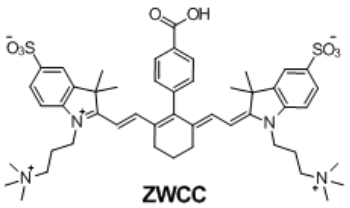

ZWCC

Chemical Formula: $C_{49}H_{63}N_4O_8S_2^{+}$
Exact Mass: 899.41

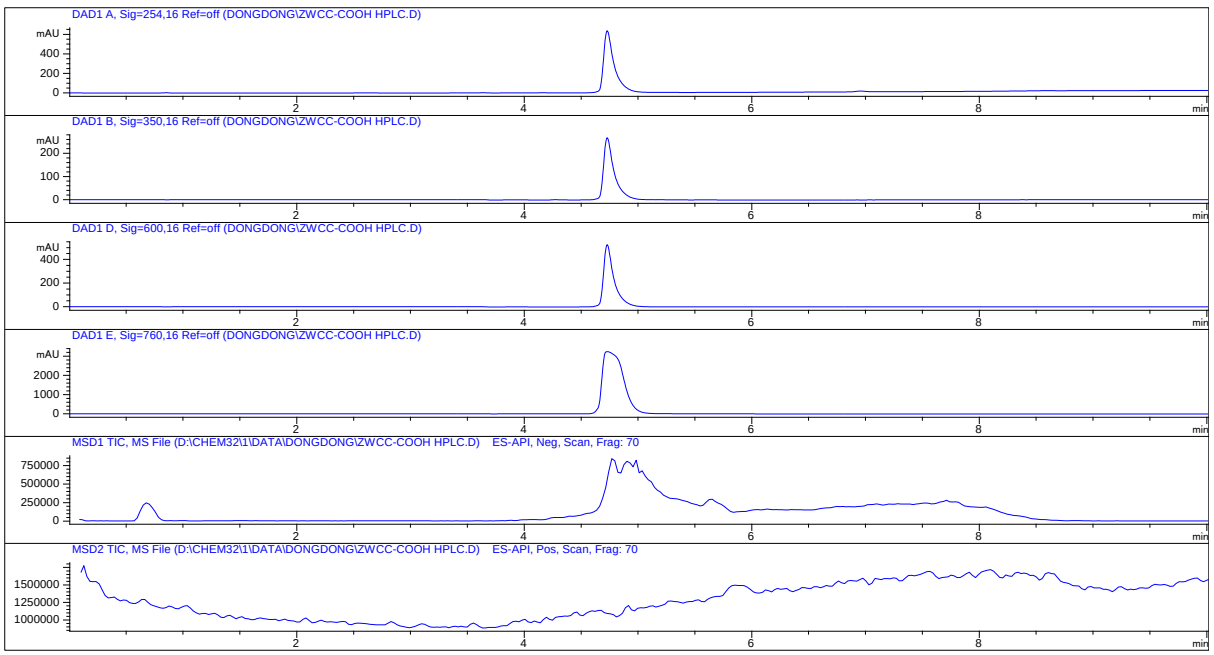

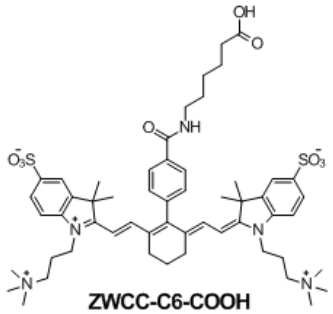

ZWCC-C6-COOH

Chemical Formula: $C_{55}H_{74}N_5O_9S_2^+$

Exact Mass: 1012.49

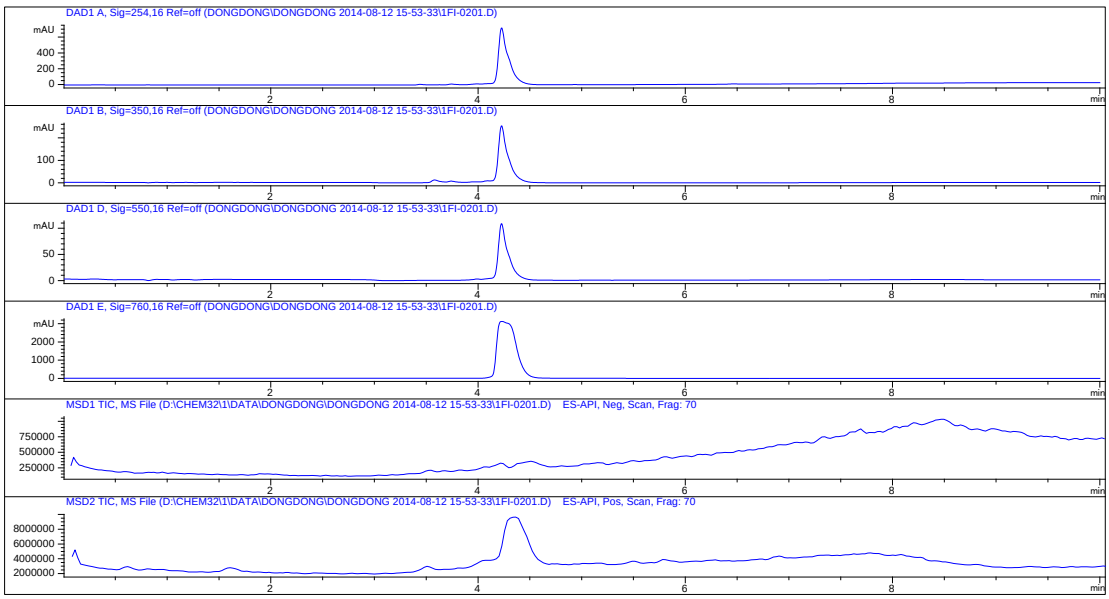

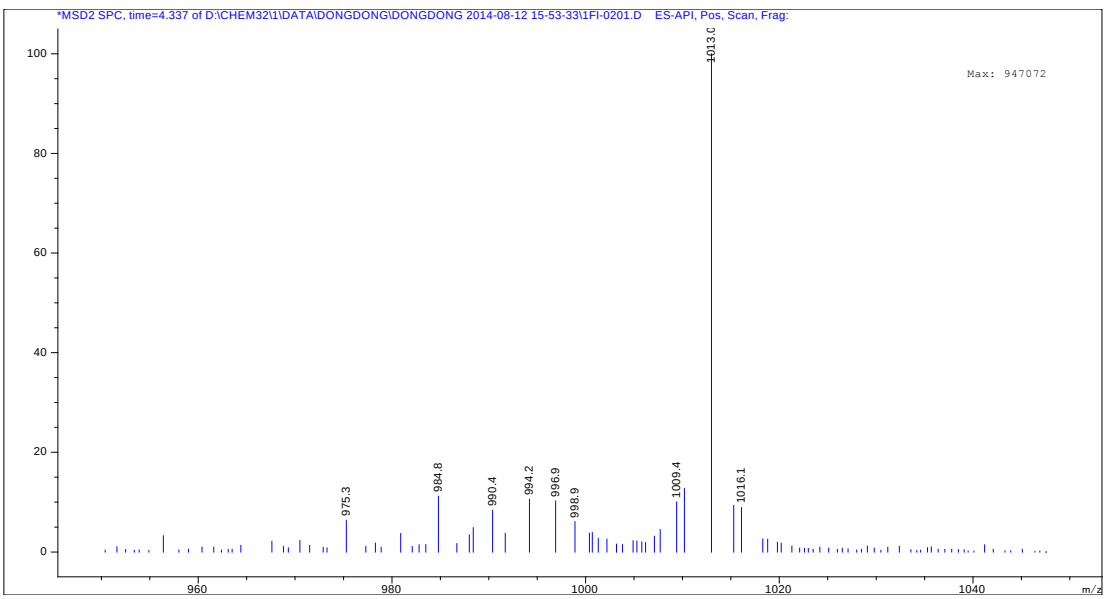

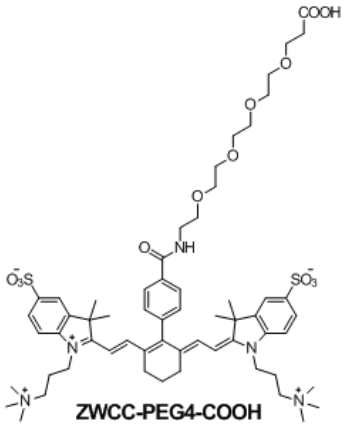

ZWCC-PEG4-COOH

Chemical Formula: $C_{60}H_{84}N_5O_{13}S_2^+$

Exact Mass: 1146.55

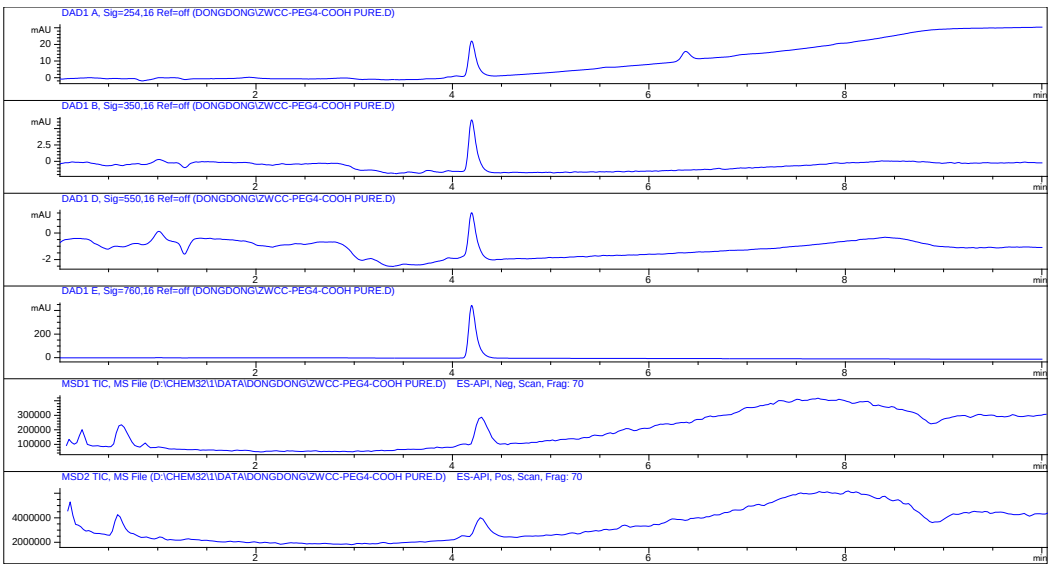

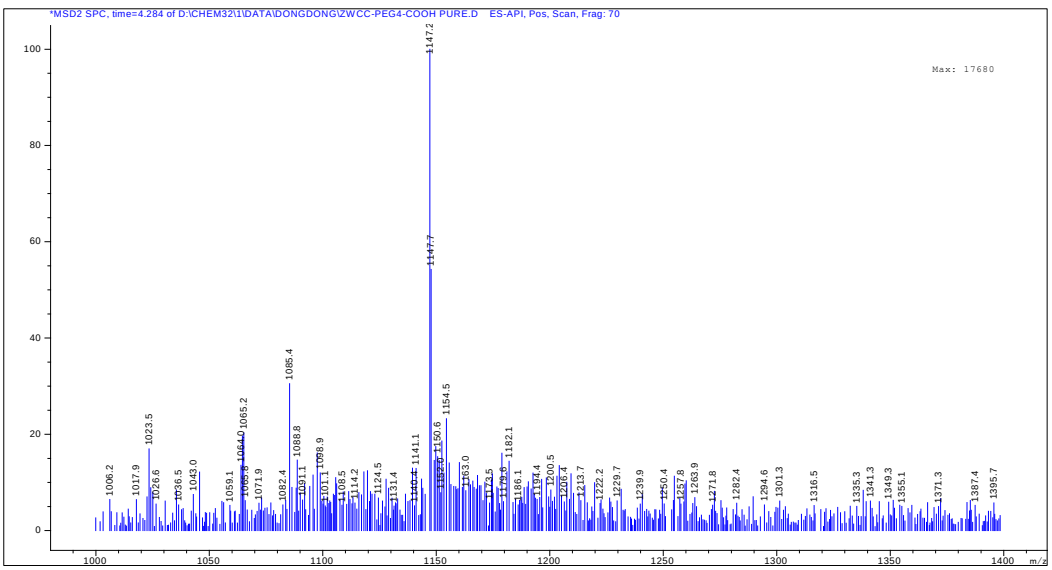

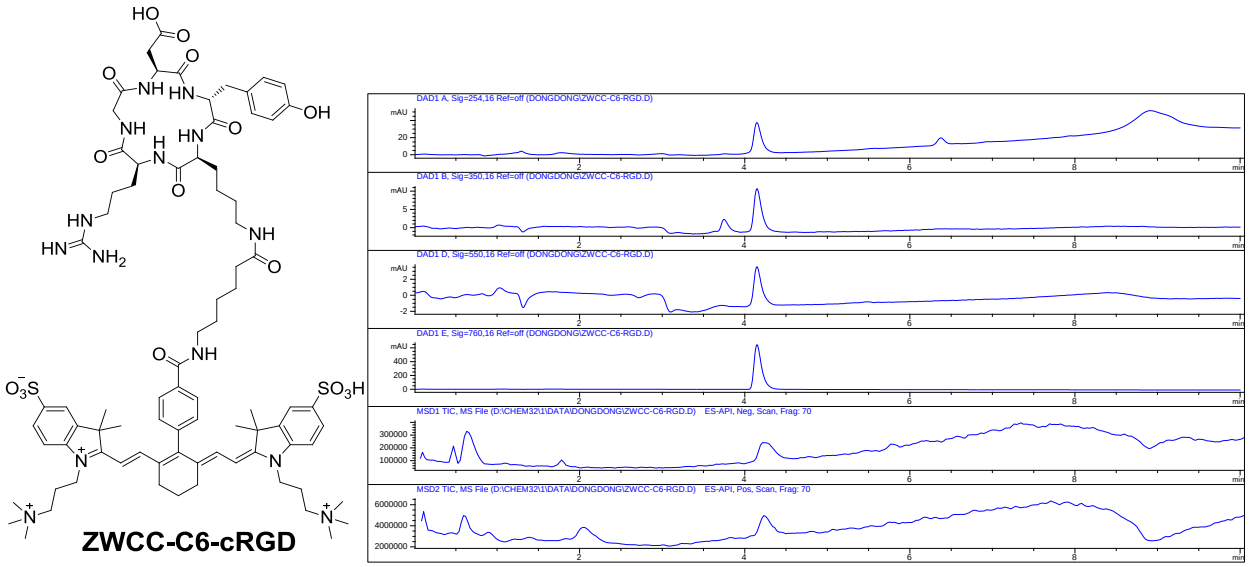

HRMS *m/z* ($C_{82}H_{114}N_{14}O_{16}S_2^{2+}$) calculated: 807.3984, found: 807.3954.

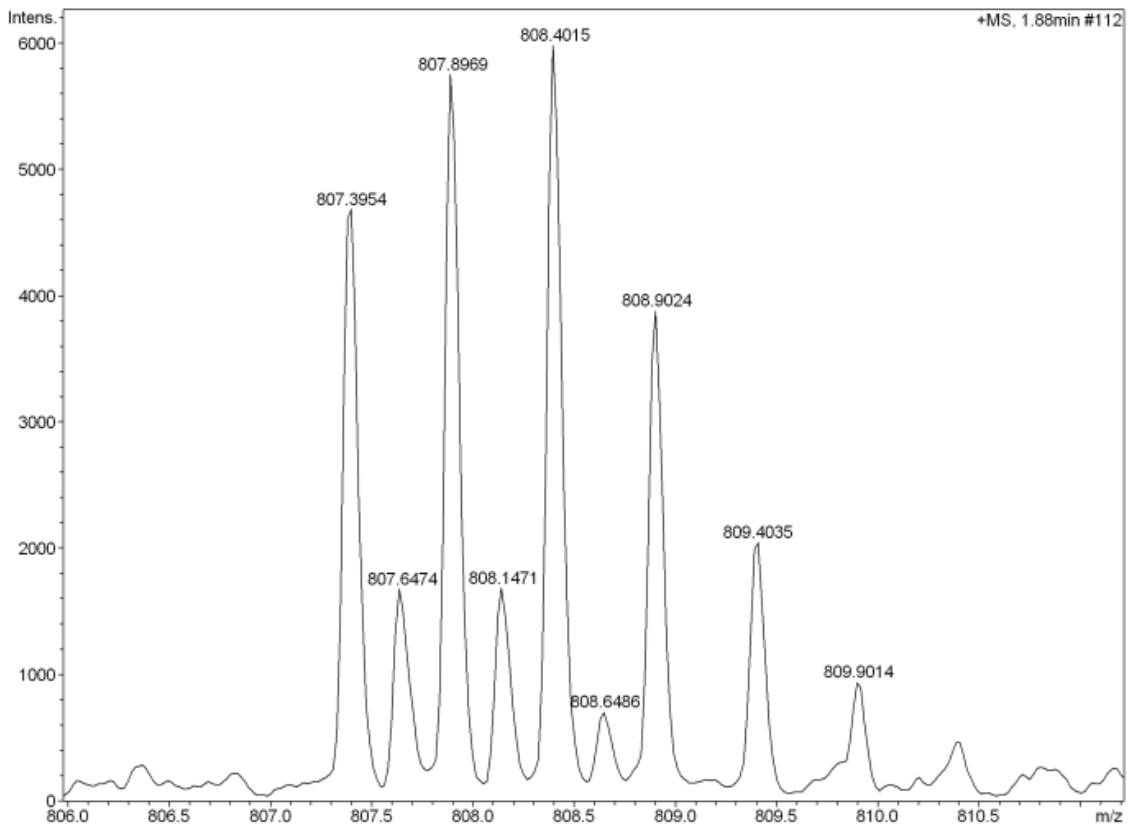

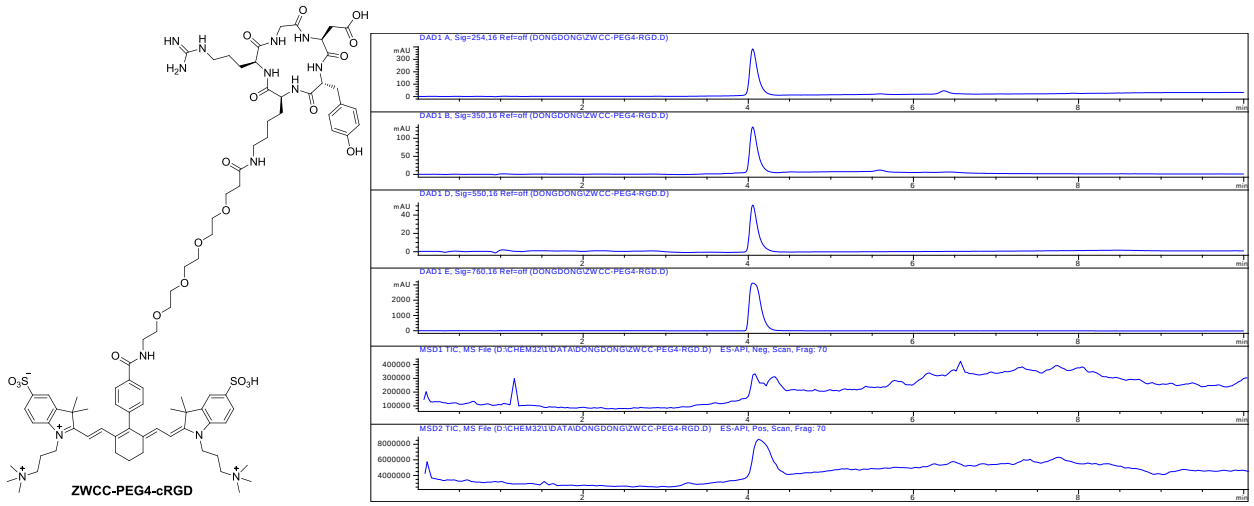

HRMS *m/z* ($C_{87}H_{124}N_{14}O_{20}S_2^{2+}$) calculated: 874.4274, found: 874.4243.

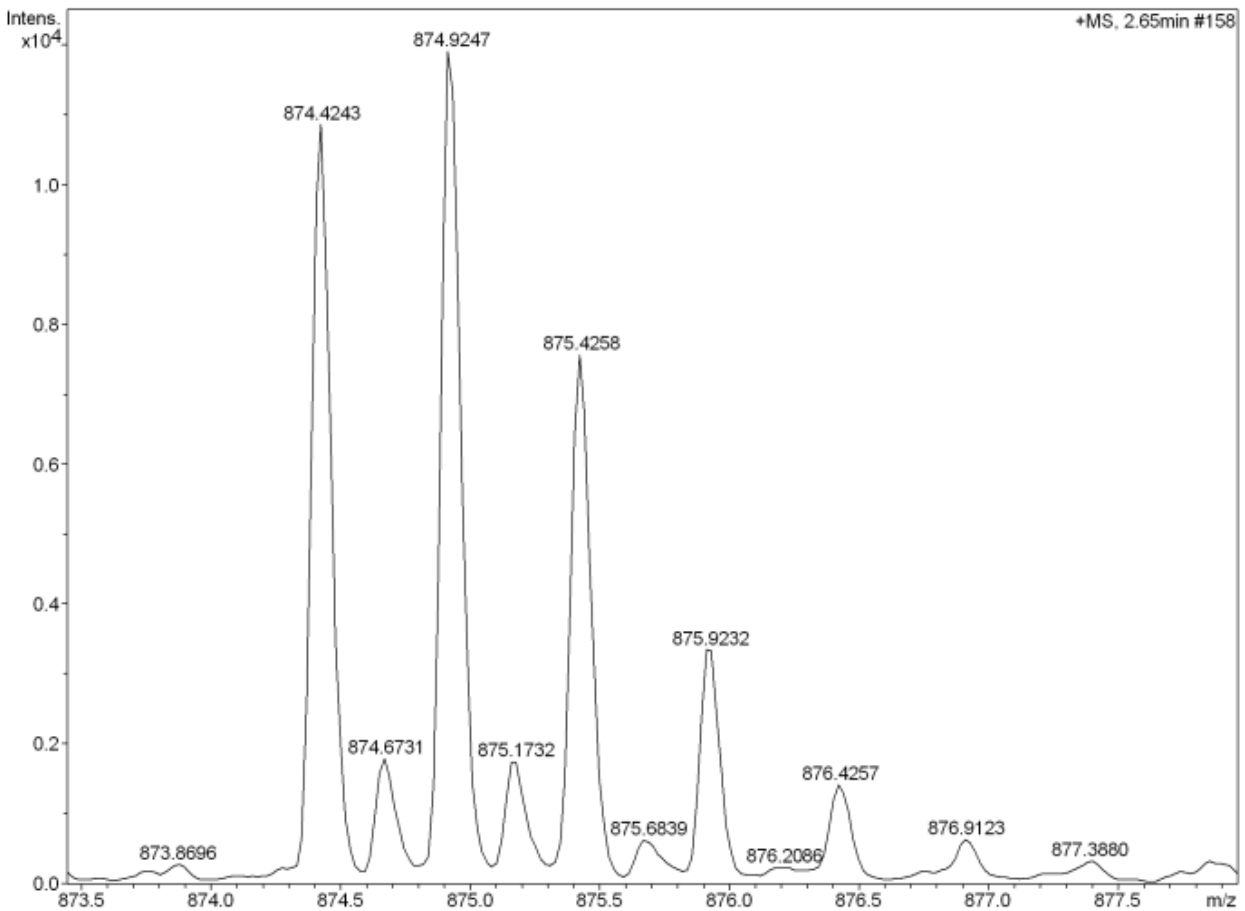

References

1. K. Licha, B. Riefke, V. Ntziachristos, A. Becker, B. Chance and W. Semmler, *Photochemistry and photobiology*, 2000, **72**, 392-398.
2. H. S. Choi, K. Nasr, S. Alyabyev, D. Feith, J. H. Lee, S. H. Kim, Y. Ashitate, H. Hyun, G. Patonay, L. Strekowski, M. Henary and J. V. Frangioni, *Angewandte Chemie*, 2011, **50**, 6258-6263.